Mass Spectrometric and Quantum Mechanical Analysis of Gas-Phase Formation, Structure, and Decomposition of Various b_2 Ions and Their Specifically Deuterated Analogs

Klaus Eckart, Max C. Holthausen,*† Wolfram Koch,* and Joachim Spiess
Department of Molecular Neuroendocrinology, Max Planck Institute for Experimental Medicine, Goettingen, Germany

B ions represent an important type of fragment ions derived from protonated peptides by cleavage of an amide bond with N-terminal charge retention. Such species have also been discussed as key intermediates during cyclic peptide fragmentation. Detailed structural information on such ion types can facilitate the interpretation of multiple step fragmentations such as the formation of inner chain fragments from linear peptides or the fragmentation of cyclic peptides. The structure of different b_2 ion isomers was investigated with collision-induced dissociations (CID) in combination with hydrogen/deuterium (H/D) exchange of the acidic protons. Special care was taken to investigate fragment ions derived from pure gas-phase processes. Structures deduced from the results of the CID analysis were compared with structures predicted on the basis of quantum chemical density functional theory (DFT) calculations to be most stable. The results pointed to different types of structures for b_2 ion isomers of complementary amino acid sequences. Either the protonated oxazolone structure or the N-terminally protonated immonium ion structure were proposed on the basis of the CID results and the DFT calculations. In addition, the analysis of different selectively N-alkylated peptide analogs revealed mechanistic details of the processes generating b ions. (J Am Soc Mass Spectrom 1998, 9, 1002–1011) © 1998 American Society for Mass Spectrometry

The analysis of the primary structure of peptides with tandem mass spectrometry was established after the introduction of desorption ionization methods, especially fast atom bombardment (FAB) to mass spectrometry [1]. These methods allow ionization of underivatized peptides, which are then subjected to collision-induced dissociations (CID). The analysis of the resulting fragmentation patterns has been used to deduce peptide sequences and is especially useful for the analysis of posttranslational modifications of peptides and proteins [2, 3]. It has been reported that peptide sequences could be assigned by the rationalization of the fragmentation resulting from peptide backbone cleavages [4, 5]. B_n ions and $y_{(N-n)}$ ions with n and N indicating the number of the current amino acid and the total number of residues of the peptide, respectively, play a key role in the interpretation of mass spectral peptide fragmentation patterns, because they represent the products of the cleavage of the amide bond n associated with N- or C-terminal charge retention, respectively (Scheme **1a**).

Knowledge on the structure and fragmentation behavior of y and b ions is of crucial importance when peptides are sequenced with mass spectrometric techniques employing consecutive fragmentation reactions such as low energy CID and multiple stage tandem mass spectrometry (MS^n) [6, 7]. Furthermore, b ions were found to be the ring opening products and major fragmentation products of protonated cyclic peptides [8]. A number of reports dealing with the structural investigations of y ions [9, 10] and b ions [10–14] appeared.

y ions were identified as N-terminally truncated protonated peptide ions [9, 10]. In contrast, an acylium ion structure (Scheme 1b) [2] was assigned to b ions. Cordero et al. demonstrated by FAB combined with CID mass spectral analysis that the structure of the Ala–Ala b_2 ion was different from the structure of the corresponding protonated diketopiperazine [10]. This observation was also reported for b_2 ions consisting of two Gly residues [11] or one Gly and one Pro residue

Address reprint requests to Dr. Klaus Eckart, Department of Molecular Neuroendocrinology, Max Planck Institute for Experimental Medicine, Hermann Rein Strasse 3, 37075 Goettingen, Germany. E-mail: eckart@mail.mpiem.gwdg.de.

* Institut für Organische Chemie, Technische Universität Berlin, Strasse des 17. Juni 135, D-10623 Berlin, Germany.

† Present address: Organisch-chemisches Institut, Universität Zürich, Winterthurerstrasse 190, CH-8057 Zürich, Switzerland.

1044-0305/98/$19.00
PII S1044-0305(98)00076-2

Received December 22, 1997
Revised May 13, 1998
Accepted May 14, 1998

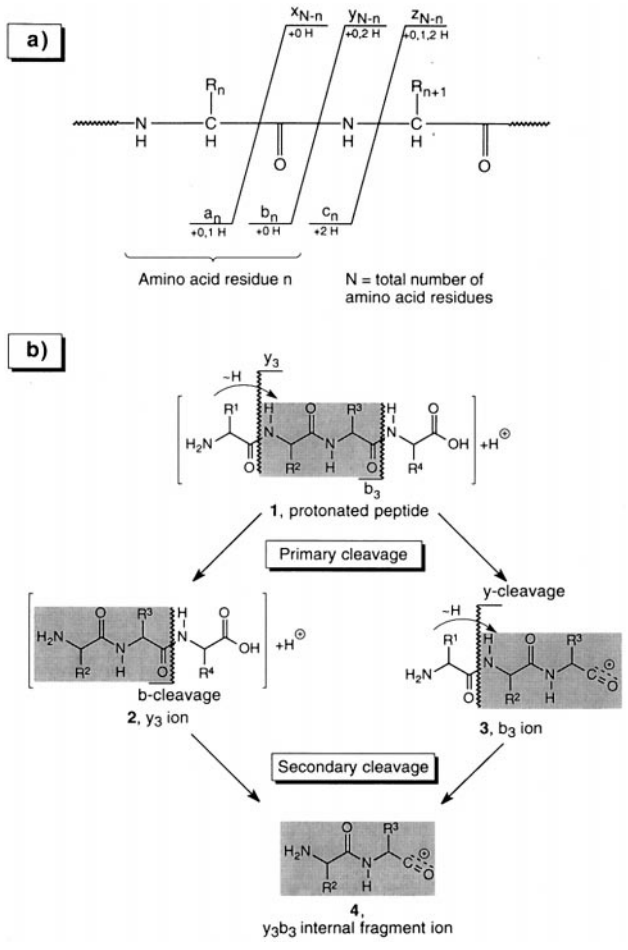

Scheme I. (**a**) Reported types of mass spectrometric peptide backbone fragmentation. (**b**) Primary and secondary amide bond cleavages of protonated peptides during mass spectrometric analysis.

[12]. The protonated oxazolone structure was proposed for the first time for the Ala–Ala b_2 ion [10]. In view of these considerations the structure of N-benzoyl glycine was investigated as a model for b ions. Identical CID mass spectra were observed for the b ion derived from N-benzoyl–Gly–OH **5** and protonated 2-phenyl-5-oxazolone **6** (Scheme **2**) [13]. This was the first experimental evidence for the oxazolone structure of a b ion. However, the N-benzoyl glycine b ion lacked the N-terminal amino group of longer b ions obtained from unmodified peptides and, therefore, could not serve as a model system for b ion structures of peptides in general. Furthermore, the investigation of isomeric b_2 ions derived from H–Gly–Pro–Gly–OH or H–Pro–Gly–Gly–OH provided evidence for differences in their structures [15].

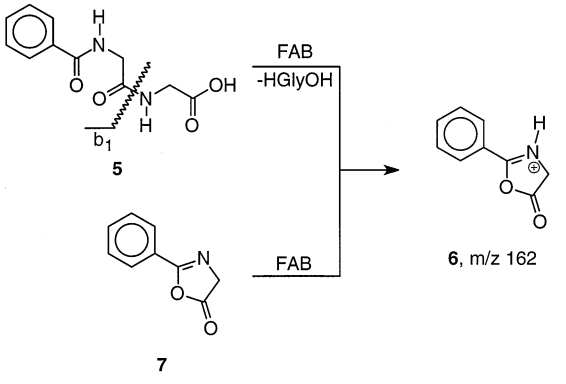

Scheme 2. Formation and identification of protonated 2-phenyl-5-oxazolone from N-benzoyl–Gly–Gly–OH.

Yaclin et al. studied the properties of a variety of b_n ions [13, 14] by kinetic energy release measurements and low energy CID. On the basis of kinetic energy release measurements they concluded that b_n ions with $n = 3, 4$ also exhibit a protonated oxazolone structure. The release of a kinetic energy ($T_{1/2}$) of 0.3–05. eV correlated with the energy difference between the unstable acylium ion (b_n) and the resulting a_n ion and neutral CO [13]. However, this observation did not provide evidence for the oxazolone structure because kinetic energy release measurements reflect the properties of unstable ions in the gas phase [16]. A CID based comparison of these b_n ions with oxazolone reference compounds was not possible because of the lack of oxazolones other than 2-phenyl-5-oxazolone. Nold et al. applied high energy CID to protonated 2-phenyl-5-oxazolone **6** and found a significant signal for loss of CO_2 [17]. They analyzed the b_2 ions with the sequence Gly–Leu and Leu–Gly for this fragmentation and found signals of relatively low abundance.

Investigation of the mechanism of b ion formation may help to understand the b ion structures. The investigation of selectively N-alkylated peptides after protonation in the gas phase [18, 19] showed a clear preference for the formation of the b ions having the N-alkylated amino acid residue in the C-terminal position. On this basis, the relative abundance of the various b_n ions of selectively N-alkylated analogs of the peptide [Pyr^6]–substance P^{6-11} (Pyr^6–SP^{6-11}) have been analyzed in the present study with tandem mass spectrometry. In addition, hydrogen/deuterium (H/D) exchange of the acidic hydrogen atoms [9, 20–22] was performed with a number of tripeptides and a mechanism for b ion formation was proposed on these experimental data.

Various heteromeric b_2 ions composed of two different amino acids such as Ala, Gly, Pro, and N-methyl glycine (sarcosine, Sar), were chosen as models for b ions containing amino acid residues with uncharged side chains. The structures were analyzed with CID of the ions obtained with electrospray (ES). Especially, the comparison of the CID mass spectra of b_2 ions with reversed amino acid sequences was used to obtain evidence for b ion structures. Furthermore, hydrogen/deuterium (H/D) exchange of the acidic hydrogen atoms [9, 20–22] was carried out in order to study the mechanisms of b_2 ion decomposition. Finally, the structures deduced from the experimental results were analyzed with quantum chemical calculations for their relative energetic stability.

Experimental

All mass spectral data were recorded on a Micromass AutoSpec-T tandem mass spectrometer equipped with a 3 in. focal plane detector. Data were recorded and processed using the OPUS data system.

ES Mass Spectra

The Micromass ES interface and the operation conditions were recently described [23]. The interface was additionally equipped with a skimmer lens. The ions were accelerated between the skimmer and the source slit with a potential difference of 4 kV. The spray chamber was heated to 30°C. Higher temperatures were avoided to prevent heat-induced molecular ion fragmentation. The sampling cone voltage and skimmer lens voltage were initially adjusted to 0 V above the skimmer potential ("*lower values*"). This setting minimized the fragmentation of the molecular ions. An optimal yield of fragment ions was achieved with the sampling cone and the skimmer lens set to 50 and 60 V, respectively, above the skimmer potential ("*higher values*"). These settings provided the best compromise between high yields of fragments by collisions between the sampling cone and the skimmer (CSCID) and unwanted scattering of the ion beam. Samples were delivered by loop injection as previously described [23]. The peptide samples were dissolved to a final concentration between 0.1 and 1 mg/ml (0.5–5 mM) in a mixture of 49.5% methanol, 49.5% water, and 1% acetic acid.

FAB Mass Spectra

Samples were ionized with a Cs^+ primary ion beam of 20 keV translational energy (12 keV effective translational energy) and 1–2 μA emission. The secondary ions were accelerated with 8 kV at a source housing pressure less than 5×10^{-6} mbar. The Pyr^6–SP$^{6-11}$ analogs were dissolved in 1 μL formic acid and mixed with 5 μL glycerol. One μL of this solution was applied to the stainless steel probe tip.

CID Mass Spectra

CID mass spectra were recorded on the array detector. The parent ion beam was focused through the collector slit of MS1 with a mass resolution of 2000. The array detector was set to a 15° angle resulting in a mass ratio of 1.1:1. The gas cell was operated at 50% of the ion energy potential, and the parent ion beam was attenuated to 30% intensity with approximately 2×10^{-6} mbar helium. The molecular ions of the Pyr^6–SP$^{6-11}$ analogs were fragmented with 2.5×10^{-6} mbar argon instead of the collision gas helium.

H/D Exchange

Each peptide (100 μg) was dried in a speed vac concentrator, dissolved in 100 μL of a mixture of 49.5% deuterium oxide (99.8% D), 49.5% methanol d_1 (99.5% D), and 1% acetic acid d_1 (99.5% D). After 2 h of incubation at room temperature, the samples were dried again and finally dissolved in 100 μL of the solvent described above. Deuterated peptides were delivered in the deuterated solvent. The yield of deuteration of peptides was between 80% and 90% depending on the number of acidic hydrogens. For MS/MS experiments the completely exchanged parent ion was selected with the first MS and selectively subjected to CID.

Peptides

Peptides were purchased from Bachem AG Heidelberg. The samples were used as received. Pro–Gly–β-naphthylamide was synthesized from tBoc–Pro–OSu and Gly–β-naphthylamide also obtained from Bachem. The Pyr^6–SP$^{6-11}$ analogs were synthesized by Professor Gilon (Hebrew University of Jerusalem, Israel). The structures of these peptides were confirmed earlier by a combination of mass spectrometry and amino acid analysis [18, 24].

Quantum Chemical Calculations

The global minimum in the conformational space of each isomer was located using the conformational analysis routine of the program Spartan 3.0. [20]. All flexible bonds in each structure were systematically rotated in 60° increments and the resulting geometries were optimized at the semiempirical PM3 level of theory [25]. The geometries of the resulting structures were reoptimized employing approximate density functional theory [26] using the DGauss program [27]. The BLYP functional was employed, which includes nonlocal corrections for exchange [28] and correlation [29]. For these calculations a polarized valence double zeta basis set was used in combination with a pseudopotential for the 1*s* electrons of C, O, and N (DZVP), as implemented in DGauss. All energies and structures discussed refer to this level of theory. Structures appearing with a computed energy difference of less than approximately 15 kJ/mol cannot safely be distinguished in their stability because of the expected level of accuracy provided by the BLYP calculations.

Results

Mechanism of b Ion Formation

The influence of amide bond protonation on b ion formation was investigated with the selectively alkylated analogs of the peptide Pyr^6–SP$^{6-11}$ (Table 1). These peptides are especially well suited for such studies

Table 1. Change in the relative abundance of b_n ions (sum of b ion current is normalized to 100%) of the CAD mass spectra induced by selective N-alkylation of the Pyr^6–SP^{6-11} analogs

Pyr^6–SP^{6-11} analog	b_2 ion (%)	b_3 ion (%)	b_4 ion (%)	b_5 ion (%)
Pyr–Phe–Phe–Gly–Leu–$MetNH_2$	7.7	14.4	29.8	48.1
Pyr–**NMePhe**–Phe–Gly–Leu–$MetNH_2$	**68.0**	2.7	8.9	20.4
Pyr–Phe–**NMePhe**–Gly–Leu–$MetNH_2$	3.7	**73.5**	5.9	16.9
Pyr–Phe–**NEtPhe**–Gly–Leu–$MetNH_2$	2.5	**82.0**	4.9	10.6
Pyr–Phe–**NPrPhe**–Gly–Leu–$MetNH_2$	0.9	**84.0**	2.5	12.6
Pyr–Phe–Phe–**Sar**–Leu–$MetNH_2$	4.9	3.5	**69.4**	22.2
Pyr–Phe–Phe–Gly–**NMeLeu**–$MetNH_2$	3.6	4.5	2.6	**89.3**

because of the missing N-terminal amino group. Thus, no competition between the amide bond and the N-terminal amino group for the proton added during ionization is possible and the effect of amide bond protonation to b_n ion formation can be studied without such interferences. The enhanced abundance of the b_n ions formed by cleavage of the C-terminal amide bond of the N-alkylated amino acids was originally observed in the FAB mass spectra of the selectively alkylated analogs of the peptide Pyr^6–SP^{6-11} [18] and was even more pronounced in the CID mass spectra of these peptides (Table 1). N-alkylation of the amino acid residue *n* resulted in a dramatic increase of the relative abundance of the b_n ion. Only a minor increase was found when methyl was replaced by ethyl or propyl.

Deuteration of the acidic hydrogen atoms [9, 20–22] and CID mass spectral analysis was carried out with all peptides used as precursors for the b_2 ions investigated (Tables 2 and 3). No scrambling between acidic and nonacidic hydrogen atoms during the formation of b ions was observed. In general, the b ions contained the number of acidic hydrogens as deuterium atoms, whereas the neutral C-terminal fragment carried the additional deuterium atom added by ionization.

On the basis of the above observations, a mechanism for b ion formation was proposed and exemplified on the tripeptide H–Gly–Ala–Gly–OH **8** (Figure 1). The carbonyl oxygen of the amide bond covering the mostly basic α-amino group was prefereably protonated/deuterated [30]. This oxygen attacked the next C-terminally located carbonyl carbon atom because of its increased nucleophilicity and ejected the neutral H–Gly–OH **9** associated with the formation of the protonated oxazolone **10**. During this process the hydrogen/deuterium atom was transferred to the amino group of the C-terminal Gly residue **9**, and the amide bond was cleaved. Despite this preferred protonation site, the other amide bond and the N-terminal amino group were also protonated to a certain extent, as could be deduced from the occurrence of the Gly a_1 and y_3a_3 immonium ions (*m*/*z* 30) [31–33]. It was concluded that the proton may migrate along the peptide backbone through hydrogen shifts between the carbonyl oxygens.

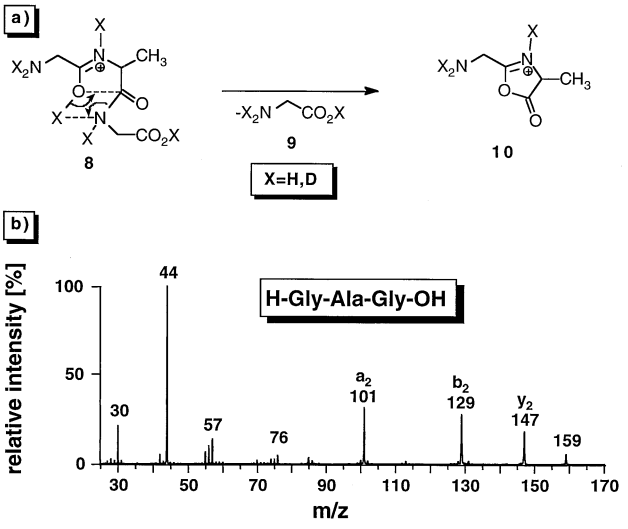

Figure 1. (**a**) Proposed mechanism for the formation of b ions from protonated peptides. (**b**) CAD mass spectrum of protonated H–Gly–Ala–Gly–OH.

Table 2. Peptides used as precursors of heteromeric b_2 ions and their cyclic isomers

Target peptide ion	*m*/*z*	Peptide precursor
Ala–Gly b_2 ion	129	H–Ala–Gly–Gly–OH
Gly–Ala b_2 ion	129	H–Gly–Ala–Gly–OH
c[Ala–Gly] + H^+	129	c[Ala–Gly]
Gly–Sar b_2 ion	129	H–Gly–Sar–Sar–OH
Sar–Gly b_2 ion	129	H–Sar–Gly–Gly–OH
Gly–Pro b_2 ion	155	H–Gly–Pro–Gly–OH
Gly–Pro b_2 ion	155	H–Gly–Pro–β-naphthylamide
Pro–Gly b_2 ion	155	H–Pro–Gly–Gly–OH
Pro–Gly b_2 ion	155	H–Pro–Gly–β-naphthylamide
c[Gly–Pro] + H^+	155	c[Gly–Pro]

Table 3. Peptides used as precursors of homomeric b_2 ions and their cyclic isomers

Target peptide ion	*m*/*z*	Peptide precursor
Gly–Gly b_2 ion	115	H–Gly–Gly–Gly–OH
Gly–Gly b_2 ion	115	H–Gly–Gly–Ala–OH
Gly–Gly b_2 ion	115	H–Gly–Gly–β-naphthylamide
c[Gly–Gly] + H^+	115	c[Gly–Gly]
Ala–Ala b_2 ion	143	H–Ala–Ala–Gly–OH
Ala–Ala b_2 ion	143	H–Ala–Ala–Ala–OH
Ala–Ala b_2 ion	143	H–Ala–Ala–β-naphthylamide
c[Ala–Ala] + H^+	143	c[Ala–Ala]

Characterization of Isomeric b_2 Ions by Their CID Mass Spectra

The ES mass spectra of the peptides used for the generation of the b_2 ions (Table 2) were recorded with the "*low settings*" and the "*high settings*" of the sampling cone and the skimmer lens voltage as described in the Experimental Procedures. In addition, the ES interface was operated at low temperature to prevent heat-induced fragmentation. Depending on the stability of the peptide molecular ion, the relative intensity of the most abundant fragment varied between 0.1% and 5% with the *low settings* of the sampling cone and skimmer lens voltages. For all peptides, the intensity of the most abundant fragment ion was enhanced by a factor of 5 to 10 compared to the intensity of the molecular ion when the *high settings* were used instead of the *low settings*. This effect demonstrated that the peptide fragments were produced by gas-phase dissociations and, therefore, those ions could be used as reference ions for MS^n investigations of fragment ions obtained in the collision cell of a sector tandem mass spectrometer [17, 34, 35] or the cell in FTICR or ion trap mass spectrometers [7].

The CID mass spectra of the heteromeric b_2 ions listed in Table 2 were obtained after ES CSCID fragmentation. In general, b_2 ions of the same amino acid sequence derived from precursor peptides carrying a different C-terminal leaving group such as Gly–OH, Ala–OH, or β-naphthylamide (Tables 2 and 3), exhibited identical CID mass spectral patterns.

The CID mass spectra of the isomeric b_2 ions of Ala and Gly were not changed to a great extent when Ala was replaced by the isomeric Sar residue in Gly–Ala (Figure 2a, b) as well as Ala–Gly (Figure 4c, d). All CID mass spectra exhibited an abundant signal for the loss of CO (m/z 101). The Ala or Sar immonium ion fragment (m/z 44) [31, 32] represented the base peak in these spectra and the b_2 ion isomers having Gly in the N-terminal position produced additionally an abundant Gly a_1 immonium ion fragment (m/z 30) [31, 32]. No evidence for the formation of the diketopiperazine could be found when the CID mass spectrum of protonated c[Ala–Gly] (data not shown) was compared with the CID mass spectra in Figure 2a, c.

The CID mass spectra were also screened for the appearance of a fragment ion representing the loss of CO_2, which may be useful to identify the protonated oxazolone structure [17]. The fragment ion m/z 71 (3%, Figure 3a) in the CID mass spectrum of the Gly–Gly b_2 ion was shifted after H/D exchange to m/z 72. In the case of a CO_2 loss this signal had to be shifted to m/z 74. A similar observation was made for m/z 99 of the b_2 ion of Ala–Ala (2%, Figure 3b), which was shifted to m/z 101 after H/D exchange. No significant signals corresponding to the loss of CO_2 were found in the CID mass spectra of the b_2 ions of the Gly–Ala and the Gly–Sar isomers (m/z 85, Figure 2), and the Gly–Pro isomers (m/z 111, data not shown). In addition, the CID mass spectrum of protonated 2-phenyl-5-oxazolone **6** formed by loss of H–Gly–OH from protonated Hippuryl-Gly–OH **5** (Scheme **2**) was reproduced with the CID method used in this paper. A mass spectral fragmentation pattern similar to that reported by Nold et al. [17] except for the loss of CO_2 was found (Figure 4). Thus, the loss of CO_2 could not be used as an indicator for the protonated oxazolone structures analyzed with the CID method used in the present paper.

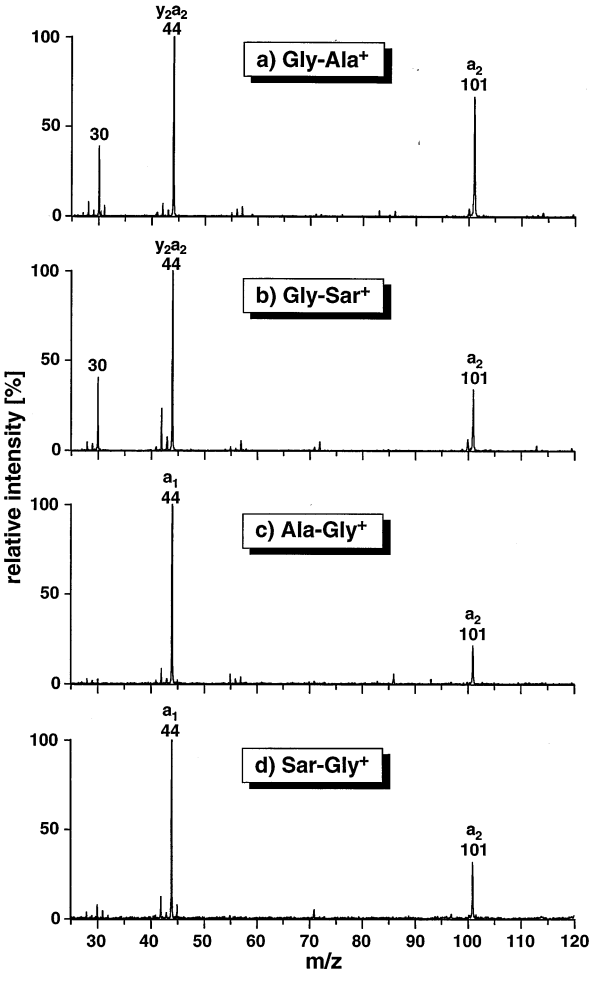

Figure 2. CAD mass spectra of isomeric $C_5H_9N_2O_2^+$ ions of ES-protonated and CS CAD-fragmented (**a**) H–Gly–Ala–Gly–OH, (**b**) H–Gly–Sar–Sar–OH, (**c**) H–Ala–Gly–Gly–OH, and (**d**) H–Sar–Gly–Gly–OH.

The protonated oxazolone structure was accepted so far as the stable structure of b ions [10, 13, 14, 17, 33]. This structure was also expected from the mechanism presented above (Figure 1). However, the different CID mass spectral patterns of the isomeric b_2 ions could not be explained on this basis. Thus, fragmentation of the Gly–Ala b_2 ion gave rise to the y_2a_2 immonium ion fragment at m/z 44 derived from the C-terminal Ala residue (Figure 2a). In contrast, the isomeric Ala–Gly b_2 ion did not form an y_2a_2 immonium ion fragment at m/z 30 derived from the C-terminal Gly residue (Figure 2c). Such corresponding a_1 fragment ion signal was observed in case of the N-terminal localization of the

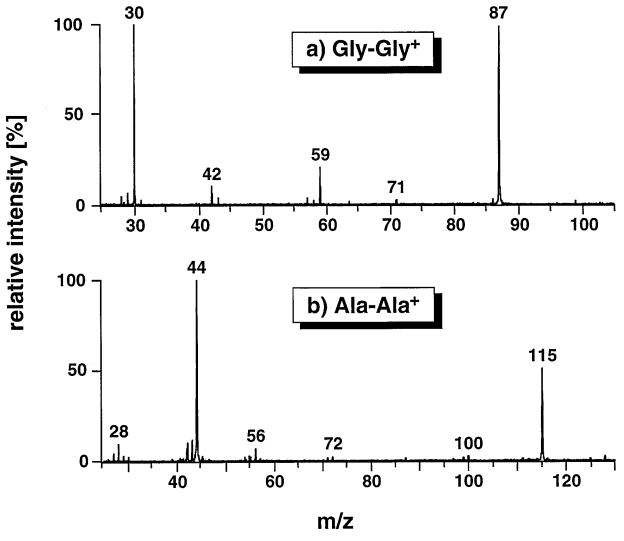

Figure 3. CAD mass spectra of the $C_4H_7N_2O_2^+$ ion of ES-protonated and CS CAD-fragmented (**a**) H–Gly–Gly–Gly–OH and the $C_6H_{11}N_2O_2^+$ ion of ES-protonated and CS CAD-fragmented (**b**) H–Ala–Ala–Ala–OH.

Gly residue in the Gly–Ala b_2 ion. Because this difference in the fragmentation patterns could not be explained by the protonated oxazolone structure for both b_2 ion isomers, it was speculated that an alternative structure with N-terminal charge localization could be valid for the Ala–Gly b_2 ion. This consideration was used as a basis for the DFT calculations.

Analysis of Stable b_2 Ion Structures by DFT Calculations

Initially, different types of possible N-terminally charged b_2 ions structures were analyzed with DFT calculations. The protonated immonium ion **13** was found to be by far the most stable isomer. The protonated Ala–Gly diketopiperazine **11**, the protonated oxazolone structures **10** and **12** and immonium ion structures **10** and **13** of the Ala–Gly b_2 ions were than compared for their energetic stability on the basis of the results of DFT calculations. The protonated Ala–Gly diketopiperazine **11** and the immonium ion structure of the Ala–Gly isomer **13** were the energetically most

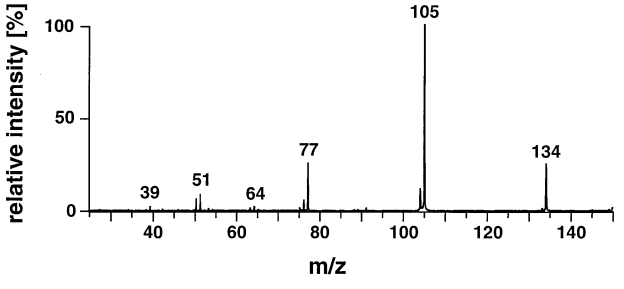

Figure 4. CAD mass spectrum of the $C_9H_8N_1O_2$ ion of ES-protonated and CS CAD-fragmented Hippuryl–Gly–OH.

Table 4. Structures and relative energies of the most stable isomeric $C_5H_9N_2O_2^+$ ions from peptides containing Ala and Gly

Ala-Gly protonated diketopiperazine	Ala-Gly b_2 ion structures	Gly-Ala b_2 ion structures	
11 0 kJ/mol	**12** 42 kJ/mol	**10** 31 kJ/mol	protonated oxazolone structures
	13 7 kJ/mol	**14** 46 kJ/mol	immonium ion structures

stable isomers (Table 4), whereas the difference of 7 kJ/mol between these structures was not significant, because a difference of less than 15 kJ/mol is not significant for the level of theory used in the DFT calculations. The oxazolone structures of the Gly–Ala isomer **10** and the Ala–Gly isomer **12** turned out to be less stable than the protonated diketopiperazine **11** by a difference of 31 and 42 kJ/mol, respectively (Table 4). The immonium ion structure of the Gly–Ala isomer **14** was 46 kJ/mol less stable than the protonated diketopiperazine **11** (Table 4). For the Ala–Gly b_2 ion isomer the immonium ion form **13** was 35 kJ/mol more stable than the protonated oxazolone form **12**, whereas the immonium ion form **14** was 15 kJ/mol less stable than the protonated oxazolone **10** of the Gly–Ala b_2 ion isomer. Furthermore, the protonated diketopiperazine **11** was excluded as b_2 ion structure by the CID mass spectral analysis. Thus, the DFT calculations matched the predictions from the experimental data. In contrast to these findings, the protonated oxazolone and immonium ion structure of the Gly–Gly b_2 ion were less stable than the protonated Gly–Gly diketopiperazine by 39 and 40 kJ/mol, respectively. The unsignificant energetic difference of 1 kJ/mol did not allow a distinction between the oxazolone and immonium ion structure of the Gly–Gly b_2 ion by DFT calculations.

A possible mechanism for the formation of the immonium ion type b_2 ions is outlined for the Ala–Gly b_2 ion (Scheme **3**). The protonated oxazolone **12** may undergo ring opening immediately after its formation to form the acylium ion transition state **15**. This acylium ion can be stabilized by a hydrogen bridge in the N-terminal Ala residue. The α-proton of the Ala residue is transferred in a second step to the free carbonyl group resulting in the formation of the immonium ion **13**. The possibility of two hydrogen bridges and a wide distribution of the positive charge in the more basic amino acid residue are the factors stabilizing the immonium ion **13** over the protonated oxazolone **12** by 35 kJ/mol. It is speculated that the hydrogen bridge in **15** may prevent formation of the protonated diketopiperazine **11**. However, all experimental data reported so far leave

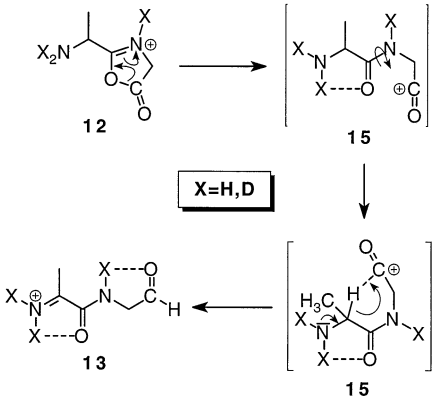

Scheme 3. Formation of iommonium ion type b_2 ions via an acylium ion transition state from protonated oxazolone type b_2 ions.

no doubt that b_2 ions did not undergo rearrangement to the isomeric diketopiperazine [10–13, 17].

Pathways of b_2 Ion Dissociation Monitored by H/D Exchange

The CID mass spectra of deuterated b_2 ions (Table 5) showed no significant H/D scrambling with respect to the a_1 and y_2a_2 immonium ion fragments of the amino acid residues. The primary amines of Ala and Gly contained two deuterium atoms, whereas the secondary amines of Sar and Pro contained one deuterium atom. This observation demonstrated that the y_2a_2 immonium ion fragments **19** of the amino acid residues located at the C-terminal position in the b_2 ion **16** were formed in association with the transfer of one acidic hydrogen from the N-terminal residue (Scheme **4**).

Table 5. Changes in mass-to-charge ratio and relative intensity of the CO loss and the amino acid immonium ions after H/D exchange in the CAD mass spectra of various b_2 ions

b_2 ion	Nondeuterated fragments	Deuterated fragments
Gly–Gly	*m/z* 87 (95%)	*m/z* 90 (90%)
Gly–Gly	*m/z* 30 (100%)	*m/z* 32 (100%)
Ala–Ala	*m/z* 115 (50%)	*m/z* 118 (20%)
Ala–Ala	*m/z* 44 (100%)	*m/z* 46 (100%)
Gly–Ala	*m/z* 101 (60%)	*m/z* 104 (70%)
Gly–Ala	*m/z* 44 (100%)	*m/z* 46 (90%)
Gly–Ala	*m/z* 30 (40%)	*m/z* 32 (100%)
Gly–Sar	*m/z* 101 (35%)	*m/z* 103 (18%)
Gly–Sar	*m/z* 44 (100%)	*m/z* 45 (52%)
Gly–Sar	*m/z* 30 (44%)	*m/z* 32 (100%)
Gly–Pro	*m/z* 127 (75%)	*m/z* 129 (65%)
Gly–Pro	*m/z* 70 (100%)	*m/z* 71 (77%)
Gly–Pro	*m/z* 30 (55%)	*m/z* 32 (100%)
Ala–Gly	*m/z* 101 (23%)	*m/z* 104 (25%)
Ala–Gly	*m/z* 44 (100%)	*m/z* 46 (100%)
Sar–Gly	*m/z* 101 (37%)	*m/z* 103 (28%)
Sar–Gly	*m/z* 44 (100%)	*m/z* 45 (100%)
Pro–Gly	*m/z* 127 (28%)	*m/z* 129 (35%)
Pro–Gly	*m/z* 70 (100%)	*m/z* 71 (100%)

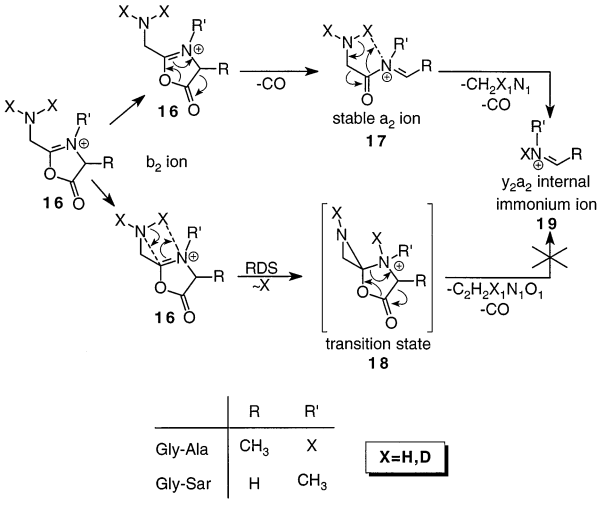

Scheme 4. High energy collision induced fragmentation route for the formation of the C-terminal amino acid immonium ions from protonated oxazolone type b_2 ions.

An abundant increase of the a_1 Gly immonium ion cleaved from the protonated oxazolone b_2 ions Gly–Ala, Gly–Sar, and Gly–Pro by a factor of 2.4 to 4.4 relative to the competing Ala, Sar, or Pro immonium ion fragments was observed after deuterium incorporation (Table 5). This effect was not found by CID mass spectral analysis of the corresponding a_2 ions, which were formed by CO loss of the b_2 ions [3]. Thus, the stable a_2 ion **17** of, i.e., Gly–Ala or Gly–Sar could not be an intermediate of the high energy collision-induced fragmentation of these oxazolone type b_2 ions **16** (Scheme **4**). These observations implied an initial transfer of one proton as the rate determining step (RDS) in the b_2 ions **16**, which led to the transition states **18** (Scheme **4**). The y_2a_2 immonium ions **19** were formed by ejection of neutrals $C_2H_2X_1N_1O_1$ (X = H/D) and CO from **18**. Because no isotope effect was observed with the Gly–Ala, and Gly–Sar a_2 ions **17**, it was concluded that the acidic hydrogen transfer did not occur as the RDS in the fragmentation reaction to form the y_2a_2 ion from the stable a_2 ion. A concerted mechanism would be compatible with this observation.

The mechnism for the a_1 immonium ion formation from b_2 immonium ions such as **13** was proposed on the basis of the H/D exchange results (Scheme **5**). As mentioned above, the resulting a_1 ion of Ala contained two deuterium atoms. This observation implied the transfer of one nonacidic proton located at the carbonyl

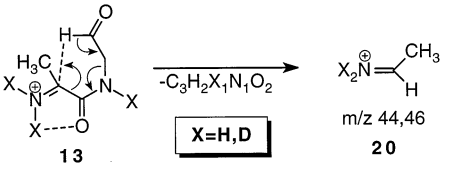

Scheme 5. Formation of a_1 ions from iommonium ion type b_2 ions.

group or at the α-carbon atom of the C-terminal Gly residue to the α-position of the N-terminal Ala residue. For sterical reasons the transfer of the carbonyl hydrogen was proposed (Scheme **5**).

Discussion

Structure of b Ions

Ambihapathy et al. reported the low energy CID breakdown graphs of the isomeric Gly–Phe and Phe–Gly b_2 ions [33]. The Gly immonium ion fragment m/z 30 (a_1 or a_2y_2) was only observed for the Gly–Phe isomer. Nold et al. showed the high energy CID mass spectra of the isomeric Gly–Leu and Leu–Gly b_2 ions [17]. The Gly immonium ion fragment m/z 30 (a_1 or a_2y_2) was again only observed in the CAD mass spectrum of in the Gly–Leu b_2 ion. Both publications confirmed independently the results presented here despite the fact that Nold et al. rationilized m/z 30 as a consecutive fragment of the Leu residue [17].

Ambihapathy et al. used the experimental design introduced by Yalcin et al. [13, 14] to justify the oxazolone structure. Since protonated 2-phenyl-5-oxazolone was used to identify the structure of the N-benzoyl–Gly b_2 ion as protonated 2-phenyl-5-oxazolone the kinetic energy release ($T_{1/2}$) associated with CO elimination from protonated 2-phenyl-5-oxazolone was used as an indicator for the protonated oxazolone structure. It was found that the $T_{1/2}$ value of approximately 0.5 eV matched the predicted energy release when the unstable acylium ion transition state dissociated into CO and the a_2 ion. Thus, such $T_{1/2}$ values hint to an acylium ion transition state [16], but not necessarily to the protonated oxazolone structure. b_2 ions of the immonium ion structure such as **13** may also lose CO via an acylium ion transition state.

The low energy CID breakdown graphs of various b_2 ions also reported by Yalcin et al. and Ambihapathy et al. [13, 14, 33] are useful to analyze the order of multiple step fragmentation reactions, but they do not provide direct evidence for a particular ionic structure. The most reliable method is the comparison of CID mass spectra of different reference ions with the ion of unknown structure. However, our attempts to synthesize reference oxazolones similar to 2-phenyl-5-oxazolone failed because of the high reactivity of the α-carbon of the amino acid in the oxazolone ring. This behavior is well explained by the use of oxazolones also named azlactones as reactive intermediates for α-alkylation of amino acids [36, 37]. Therefore, the CID-based comparison of isomeric b_2 ions and structure prediction based on DFT calculations were chosen in the present paper as tools for the structural analysis.

Nold et al. introduced the CO_2 loss, which was observed in the high energy CID mass spectrum of 2-phenyl-5-oxazolone, as an indicator for the protonated oxazolone structure [17]. This fragment was found in the CID mass spectrum of the Gly–Leu b_2 ion in convincing significance, but for the Leu–Gly isomer this fragment (m/z 127) was not significantly separated from signals occurring at m/z 124 to 126, which probably arose from Leu side chain fragmentations [38, 39]. In view of the low abundance of such signals reported for the Leu-containing b_2 ions it has to be considered that the low resolving power of the MIKES technique used by these authors hindered an unambiguous interpretation of the CID mass spectra.

Thus far, no direct evidence for the oxazolone structure of larger b ions has been provided. It must be pointed out that b ions may initially appear as protonated oxazolones. It is doubtful that this structure would describe b_n ion structures with $n \geq 3$ correctly. B ions are known to undergo metastable decompositions [40], i.e., the b_5 fragment ion with the sequence Pyr–Leu–Asn–Phe–Thr of *locust* adipokinetic hormone (AKH) was completely sequenced in a mass spectrometric experiment by metastable decompositions [41]. This observation demonstrated the presence of a nonlocalized proton in this peptide fragment, otherwise the decomposition would require high energy CID as known for remote-charge fragmentations [42]. Therefore, b_n ions for $n \geq 3$ may exist in multiple isomeric structures which allow the proton residing on carbonyl groups on the peptide backbone or the N-terminal amino group.

Relevance for Structural Analysis of Peptides

The discrimination between the N- and the C-terminal ends of inner chain fragments, which were observed for example in the low energy CID mass spectra of ES- or FAB-ionized linear peptides [43, 44] and especially for Pro containing sequences [45] (Scheme Ib) can represent a severe problem [40], because loss of a neutral amino acid residue cannot be unambiguously referred to the N- or C-terminal localization of this amino acid [40]. Analysis of a b_2 ion fragment, which represents a part of an inner chain peptide fragment, can be used to distinguish both ends of the inner chain fragment by the CID mass spectral assignment of the b_2 ion sequence.

Many fragments of protonated cyclic peptides observed in the CID mass spectra have been assigned to the b ion type [8]. One general strategy used the occurrence of b_2 ions in the CID mass spectra of cyclic peptides ionized by ES or FAB to deduce the connectivity between amino acid residues without the C- or N-terminal orientation in cyclic peptides [40]. Different strategies were provided for the discrimination between the resulting cyclic peptide sequence and retrosequence [40, 46]. The results on b_2 ions presented here can be used to determine unequivocally the correct amino acid residue orientation in cyclic peptides on the basis of each b_2 ion fragment. A similar approach was applied during the mass spectrometric investigations of the cyclic peptide gramicidin S. The CID mass spectrum of the m/z 197 fragment derived from FAB-ionized gramicidin S was compared with the CID mass spectra

of the Pro–Val and Val–Pro b_2 ions (m/z 197), which were obtained by EI of the corresponding methyl esters. On this basis the sequence Pro–Val was assigned to the m/z 197 fragment, and the entire sequence could be determined correctly [47].

Conclusion

B_2 ions containing Ala, Gly, Pro, and Sar were subjected to H/D exchange and analyzed with high energy CID. The structures suggested on the basis of these experiments were in agreement with quantum chemical calculations. The immonium ion structure of b_2 ions was attributed to heteromeric sequences carrying the more basic residue at the N-terminus, whereas the reversed sequences, which were usually observed in greater abundance than the former sequences, gave rise to stable oxazolone structures. No CO_2 loss was found for the protonated oxazolone type b_2 ion structures. The CID mass spectra of the immonium ion type b_2 ions exhibited exclusively the immonium ion fragment of the N-terminal amino acid residue, whereas the protonated oxazolone type b_2 ions provided immonium ion fragments of both amino acid residues. Thus, the N- versus C-terminus in b_2 fragment ions of different origin can be assigned. On this basis, the discrimination between the sequence and retrosequence of cyclic peptides is possible.

It was demonstrated that N-alkylation of a particular amide group enhanced the cleavage of the next C-terminally located amide bond. This observation in combination with the results of the H/D exchange experiments pointed to an initial formation of b_2 ions with the protonated oxazolone structure which may then rearrange to the immonium ion structure in the case of its greater stability.

H/D exchange experiments permitted a clear discrimination between the acidic and nonacidic hydrogens during CID. Under high energy CID conditions, the y_2a_2 immonium ion fragment of the amino acid being part of the oxazolone moiety was not formed by fragmentation via a stable a_2 ion intermediate as shown by the appearance of a primary kinetic isotope effect.

Acknowledgments

The authors thank Thomas A. Bräuninger for preliminary calculations. A generous amount of computer time and excellent service (Dr. Thomas Steinke) was provided by the Konrad–Zuse Zentrum für Informationstechnik, Berlin. Dr. Chaim Gilon (Jerusalem) is gratefully acknowledged for providing peptide samples. Dr. Peter J. Derrick (Warwick), Dr. Alex G. Harrison (Toronto), Dr. Helmut Schwarz (Berlin), Dr. Chrys Wesdemiotis (Akron), and Olaf Jahn (Goettingen) are gratefully acknowledged for their helpful discussions. We acknowledge Lars van Werven for his excellent technical help.

References

1. Barber, M.; Bordoli, R. S.; Sedgwick, R. D.; Tyler, A. N. *Nature* **1981,** *193*, 270–275.
2. Biemann, K. *Methods Enzymol.* **1990,** *193*, 455–479.
3. Papayannopoulos, I. A. *Mass Spectrom. Rev.* **1995,** *14*, 49–73.
4. Roepstorff, P.; Fohlman, J. *Biomed. Mass Spectrom.* **1984,** *11*, 601.
5. Biemann, K.; Papayannopoulos, I. A. *Acc. Chem. Res.* **1994,** *27*, 370–378.
6. Cooks, R. G.; Hoke II, S. H.; Morand, K. L.; Lammert, S. A. *Int. J. Mass Spectrom. Ion Processes* **1992,** *118/119*, 1–36.
7. March, R. E. *Int. J. Mass Spectrom. Ion Processes* **1992,** *118/119*, 71–135.
8. Eckart, K. *Mass Spectrom. Rev.* **1994,** *13*, 23–55.
9. Müller, D. R.; Eckersley, M.; Richter, W. J. *Org. Mass Spectrom.* **1988,** *23*, 217–222.
10. Cordero, M. M.; Houser, J. J.; Wesdemiotis, C. *Anal. Chem.* **1993,** *65*, 1594–1601.
11. Carrol, J. A.; Wu, J.; Do, T.; Lebrilla, C. B. *Proceedings of the 42nd ASMS Conference on Mass Spectrometry and Allied Topics*; Chicago, 1994; p 475.
12. Eckart, K.; Spiess, J. *Proceedings of the 42nd ASMS Conference on Mass Spectrometry and Allied Topics*; Chicago, 1994; p 474.
13. Yalcin, T.; Khouw, C.; Csizmadia, I. G.; Peterson, M. R.; Harrison, A. G. *J. Am. Soc. Mass Spectrom.* **1995,** *6*, 1165–1174.
14. Yalcin, T.; Csizmadia, I. G.; Peterson, M. R.; Harrison, A. G. *J. Am. Soc. Mass Spectrom.* **1996,** *7*, 233–242.
15. Eckart, K.; Holthausen, M. C.; Bräuninger, T.; Koch, W.; Spiess, J. *Proceedings of the 43rd ASMS Conference on Mass Spectrometry and Allied Topics*; Atlanta, 1995; p 1046.
16. Grützmacher, H.-F. *Int. J. Mass Spectrom. Ion Processes* **1992,** *118/119*, 825–855.
17. Nold, M. J.; Wesdemiotis, C.; Yalcin, T.; Harrison, A. G. *Int. J. Mass Spectrom. Ion Processes* **1997,** *164*, 137–153.
18. Eckart, K.; Schwarz, H.; Chorev, M.; Gilon, C. *Eur. J. Biochem.* **1986,** *157*, 209–216.
19. Vaisar, T.; Urban, J.; Nakanishi, H. *Proceedings of the 44th ASMS Conference on Mass Spectrometry and Allied Topics*; Portland, 1996; p 1241.
20. Sethi, S. K.; Smith, D. L.; McCloskey, J. A. *Biochem. Biophys. Res. Commun.* **1983,** *112*, 126–131.
21. Sepetov, N. F.; Issakova, O. L.; Lebl, M.; Swiderek, K.; Stahl, D. C.; Lee, T. D. *Rapid Commun. Mass Spectrom.* **1993,** *7*, 58–62.
22. Spengler, B.; Lützenkirchen, F.; Kaufmann, R. *Org. Mass Spectrom.* **1993,** *28*, 1482–1490.
23. Eckart, K.; Spiess, J. *J. Am. Soc. Mass Spectrom.* **1995,** *6*, 912–919.
24. Eckart, K. Ph.D. Thesis, Technical University, Berlin, 1985.
25. Stewart, J. J. P. *J. Comput. Chem.* **1989,** *10*, 209–221.
26. Seminario, J. M.; Politzer, P. *Modern Density Functional Theory. A Tool for Chemistry*; Elsevier: Amsterdam, 1995.
27. *DGauss*; Version 2.3 ed.; Cray Research Inc.: Eagan, MN, 1994.
28. Becke, A. D. *Phys. Rev. A* **1988,** *38*, 3098–3100.
29. Lee, C.; Yang, W.; Parr, R. G. *Phys. Rev. B* **1988,** *37*, 785–789.
30. Wu, J.; Lebrilla, C. B. *J. Am. Soc. Mass Spectrom.* **1995,** *6*, 91–101.
31. Johnson, R. S.; Biemann, K. *Biomed. Environ. Mass Spectrom.* **1989,** *18*, 945–957.
32. Falick, A. M.; Hines, W. M.; Medzihradszky, K. F.; Baldwin, M. A.; Gibson, B. W. *J. Am. Soc. Mass Spectrom.* **1993,** *4*, 882–893.
33. Ambihapathy, K.; Yalcin, T.; Leung, H. W.; Harrison, A. G. *J. Mass Spectrom.* **1997,** *32*, 209–215.
34. Gross, M. L.; McCrery, D.; Crow, F.; Tomer, K. B.; Pope, M. R.; Cuifetti, L. M.; Knoche, H. W.; Daly, J. M.; Dunkle, L. D. *Tetrahedron Lett.* **1982,** *23*, 5381–5384.
35. Kim, S.-D.; Knoche, H. W.; Dunkle, L. D.; McCrery, D. A.; Tomer, K. B. *Tetrahedron Lett.* **1985,** *26*, 969–972.

36. Mukerjee, A. K.; Kumar, P. *Heterocycles* **1981,** *16*, 1995–2034.
37. Mukerjee, A. K. *Heterocycles* **1987,** *26*, 1077–1097.
38. Johnson, R. S.; Martin, S. A.; Biemann, K.; Stults, J. T.; Watson, J. T. *Anal. Chem.* **1987,** *59*, 2621–2625.
39. Johnson, R. S.; Martin, S. A.; Biemann, K. *Int. J. Mass Spectrom. Ion Processes* **1988,** *86*, 137–154.
40. Eckart, K.; Schwarz, H.; Tomer, K. B.; Gross, M. L. *J. Am. Chem. Soc.* **1985,** *107*, 6765–6769.
41. Eckart, K.; Schwarz, H.; Ziegler, R. *Biomed. Mass Spectrom.* **1985,** *12*, 623–625.
42. Gross, M. L. *Int. J. Mass Spectrom. Ion Processes* **1992,** *118/119*, 137–165.
43. Tang, X.-J.; Thibault, P.; Boyd, R. K. *Anal. Chem.* **1993,** *65*, 2824–2834.
44. Bean, M. F.; Carr, S. A.; Thorne, G. C.; Reilly, M. H.; Gaskell, S. J. *Anal. Chem.* **1991,** *63*, 1473–1481.
45. Vaisar, T.; Urban, J. *J. Mass Spectrom.* **1996,** *31*, 1185–1187.
46. Eckart, K.; Schwarz, H. *Helv. Chim. Acta* **1987,** *70*, 489–498.
47. Nakamura, T.; Nagaki, H.; Kinoshita, T. *Mass Spectrosc.* **1986,** *34*, 307–319.